

Geochemistry of tourmaline-bearing granite from Maras-Jong, Terengganu, Peninsular Malaysia

AZMAN A. GHANI

Department of Geology, University of Malaya
50603 Kuala Lumpur

Abstract: The Eastern Belt Granite of Peninsular Malaysia consists mainly of I-type granites with subordinate S-type granites. The monzo- to syenogranite Maras-Jong pluton in the Eastern Belt Granite show many S-type characteristics such as presence of tourmaline, garnet, similar texture (both granites are coarse grained primary textured sometimes dominated by K-feldspar phenocrysts) and high SiO₂ contents. However, using the previous granite classification, ACNK values below 1.1 and low Al biotite content, the Maras-Jong granite can be classified as I-type granite. It is suggested that the Maras-Jong granite is a felsic I-type granite.

Abstrak: Granit Jalur Timur di Semenanjung Malaysia mengandungi batuan granit jenis I dengan sedikit jenis S. Batuan Monzogranit dan syenogranit pluton Maras-Jong di dalam Granit Jalur Timur menunjukkan banyak ciri-ciri granit jenis S seperti kehadiran mineral tourmalin, garnet, persamaan tekstur (kedua-dua granit adalah berbutir kasar bertekstur primer kadang kala didominasi oleh fenokris K-feldspar) dan kandungan SiO₂ yang tinggi. Walau bagaimanapun, menggunakan pengelasan yang terdahulu, nilai ACNK dibawah 1.1 dan mengandungi biotite kurang Al, Granit Maras-Jong boleh dikelaskan sebagai jenis I.

INTRODUCTION

Granitoid batholiths in the East Coast Province are distributed as linear masses parallel to the medial suture in Peninsular Malaysia. The province extends for a distance of 600 km and has typical exposed width of 80 km. The western margin of the province is characterized by abrupt development of granitoid along a line approximately 100 km from the medial suture. A biotite ± hornblende granodiorite to granite of variable texture is the most common rock type but a single intrusive complex may consist of rocks ranging from gabbro to granite (e.g. Jerong complex) (Cobbing *et al.*, 1992). Mafic plutons are usually the earliest in the sequence of intrusions and they occur as marginal bodies of the felsic plutons. Mafic dyke swarms mainly of doleritic composition are common.

Liew (1983) divided the Eastern Granite Province into three that is I-type granites, S-type granites and mafic rocks associated with the two granites. All the three types have different magma sources, the mafic association originate from high level fractionated components of mantle-derived primitive tholeiitic magma, the S-type granite resulting from partial melting of metasedimentary sequences under amphibolite-granulite facies condition involving muscovite and/or biotite breakdown and the I-type granite resulted from hornblende fractionation of metaluminous magma. Among the characteristics of the S-type magma in the Eastern Granite Province are high SiO₂ content (69–77%), presence of high Al biotite, ilmenite and tourmaline. The granites occur as scattered stocks and as constituent plutons of large batholiths.

Maras-Jong pluton in the Eastern Belt Granite (Fig. 1)

show many S-type characteristics such as presence of tourmaline, garnet and high SiO₂ content. The pluton is the most easterly granitic body of the Eastern Belt in the Peninsular Malaysia. The granites intruded the Sungai Perlis Beds which consists of slate, phyllite, metaquartzite and chialstolite slate. The Maras-Jong granite is divided into two units that is the granite proper and grey microgranite dyke intruded the granite. This paper will examined in detail the petrology, mineral chemistry and geochemistry of the pluton and in comparison with the Western Belt Granite.

PETROLOGY

The average modal data for Maras-Jong granite is quartz (35%), plagioclase (19%), K-feldspar (43%), biotite (4.5%) and can be classified as monzo-to syenogranite in the QAP diagram (Streckeisen 1976). Accessory minerals include apatite, garnet, tourmaline and zircon.

Large K-feldspar phenocrysts up to 3 cm long are common. In thin section most of the K-feldspar have perthitic texture. Chemical composition of the mineral shows that it contains up to 0.3% BaO and 12–16% K₂O. Plagioclases display a variety of habits (size between 0.5 mm to 2 mm). It may occur as discrete phenocrysts or as glomeroporphyritic aggregates showing resorbed outlines in the mafic members of the granites. The most common plagioclase type is oligoclase. Occasionally the crystals have corroded or cracked cores, which probably represents an early or pre-emplacement plagioclase, which was resorbed during the ascent of the magma (Mason, 1985). Thin late albitic rim sometimes can be found surrounding the plagioclase crystal. Geochemical analyses of the

plagioclase show that the mineral contain 62 to 65% SiO_2 , 22 to 24% Al_2O_3 , 8 to 9% Na_2O and up to 0.2% BaO .

Quartz in the Maras-Jong granite is mostly anhedral and generally interstitial to all other minerals, especially plagioclase and to a lesser extent to the microcline. Its also occurs as small round crystals at the margins of the plagioclase. Mymerkitic intergrowth of quartz and plagioclase is rather common. Biotite may occur as discrete plates, as ragged shreds in mafic clots and as small flakes associated with granoblastic aggregates of quartz and plagioclase. The pleochroism scheme is typically pale brown to dark brown. Available geochemical data indicate that the biotites from Maras-Jong granite (central part of the Western Belt) is different from the biotite that crystallized from peraluminous melt which is characterized by high Al_2O_3 content (17-21%). The biotite from the

Maras-Jong granite typically has 12.56-13.6% Al_2O_3 , 2.9-4.2% TiO_2 , 3.9-4.2% MgO and 8.8-9.3% K_2O

Zircon and apatite are ubiquitous accessory phases. Euhedral garnet is uncommon and only observed in rocks of leucogranitic composition. Tourmaline occurs as an interstitial mineral to plagioclase, quartz and K-feldspar. Euhedral allanite is present in several plutons and commonly show zonation. Secondary epidote, chlorite, and occasionally sphene often occur along biotite cleavages. Epidote occurs as secondary mineral associated with sericitised plagioclase and biotite.

GEOCHEMISTRY

Analytical notes

Fifteen samples of the Maras-Jong granite proper and the grey microgranite dykes were collected and analysed. The size of samples was dependent on grain size, the largest being 5 kg. Care was taken to ensure that the granites were unaltered, the state of decomposition of the feldspar being an important indicator. Major and trace element analyses were carried out on an automated Phillips PW1400 X-Ray fluorescence (XRF) spectrometer at the Victoria University of Wellington, New Zealand.

Chemical variation

Representative geochemical composition of the Maras-Jong granite is given in Table 1. Major and trace element data are plotted against SiO_2 on variation diagrams as this is the most common granite fractionation index. The Maras-Jong granite show a restricted aluminium saturation index (ASI) with molecular $\text{Al}_2\text{O}_3/\text{Na}_2\text{O}+\text{K}_2\text{O}+\text{CaO} = 0.86$ to 1.07, and therefore all the analysed samples are mildly metaluminous to peraluminous. The granites also have a variable major element chemistry ($\text{SiO}_2 = 65.57$ -74.64 wt% and $\text{Al}_2\text{O}_3 = 12.96$ -14.65 wt%). The grey microgranite has more basic composition compared to the Maras-Jong granite proper. Thus Al_2O_3 , TiO_2 , Fe (tot), MnO , MgO , Na_2O and P_2O_5 are higher in the former (Fig. 2). Infact most of the elements grey microgranite in the have different trends compared to the Maras-Jong granite. This is an evidence shows by the FeO (tot), MnO , CaO , Na_2O and K_2O . A gap occurs between the granite proper and the grey microgranite dykes from 68.1 to 71.2% SiO_2 and this may be a true gap and not related to under sampling. On the AFM plot the rocks from the Maras-Jong pluton plot at the evolved end of the calc alkaline trend. All analysed samples from the Maras-Jong granite proper have high alkali contents, with $\text{Na}_2\text{O} + \text{K}_2\text{O}$ ranges from 7.6-8.6%. The high alkali nature of the rocks is also shown on the K_2O vs SiO_2 plot (Fig. 3), where all rocks plot in the high-K calc alkali field. However, different behavior shown the grey microgranite samples. Trend of the plot is crossing a different field from calc alkali to high-k calc alkali.

Trace element variation diagrams (Fig. 4) of the Maras-Jong pluton show a gap occurs in some of the diagrams

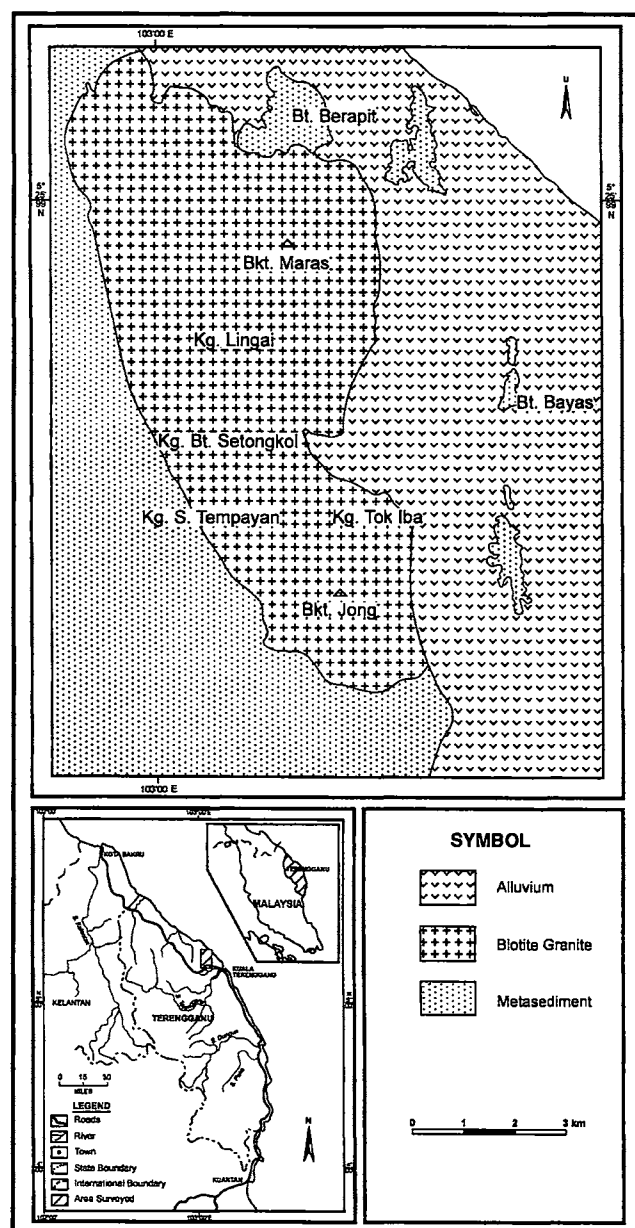


Figure 1. Location of the Maras-Jong granite and general geology of the granite and surrounding area.

Table 1. Representative geochemical analyses of major and trace elements for the Maras-Jong granite.

Sample No	Granite MBJ8	Granite MBJ9	Granite MBJ10	Granite MBJ11	Granite MBJ13	Granite MBJ18	Granite BJ1	Granite BJ2	Granite BJ3	Granite BJ4	Granite BJ6	Grey MBJ5	Grey BJ6*	Grey BJ7	Grey BJ7*
Major element in wt%															
SiO ₂	72.78	72.81	72.44	72.51	72.68	73.21	72.8	73.84	71.96	71.89	72.2	52.92	65.67	67.22	68.09
TiO ₂	0.28	0.26	0.26	0.3	0.29	0.22	0.3	0.29	0.35	0.37	0.31	1.42	0.73	0.66	0.57
Al ₂ O ₃	14.25	14	14.54	14.34	14.18	14.13	13.97	12.96	14.05	13.81	14.31	17.15	16	15.69	15.42
Fe(tot)	2.2	2.34	2.19	2.38	2.37	1.92	2.29	2.26	2.63	2.8	2.44	7.6	4.34	4.54	4.23
MnO	0.04	0.04	0.04	0.05	0.05	0.03	0.05	0.05	0.05	0.06	0.05	0.17	0.07	0.07	0.08
CaO	1.2	1.16	1.27	1.34	1.2	0.35	1.28	1.2	0.99	1.33	1.34	7.79	0.55	0.48	1.92
K ₂ O	5.04	4.91	4.73	4.61	4.93	5.21	4.86	4.24	5.59	4.58	4.62	1.5	4.87	3.41	1.42
P ₂ O ₅	0.13	0.12	0.12	0.13	0.14	0.1	0.14	0.14	0.17	0.17	0.15	0.33	0.24	0.22	0.22
MgO	0.41	0.38	0.37	0.43	0.44	0.32	0.47	0.47	0.58	0.58	0.49	5.11	1.12	1.06	0.96
Na ₂ O	3.63	3.68	3.88	3.83	3.66	3.73	3.56	3.38	3.2	3.53	3.83	3.8	4.19	4.73	5.3
Total	99.96	99.7	99.84	99.92	99.94	99.22	99.72	98.83	99.57	99.12	99.74	97.79	97.78	98.08	98.21
Trace element in ppm															
Ba	257	191	200	215	228	200	220	178	254	211	208	155	291	229	221
Ce	53	46	45	52	53	45	54	47	51	62	47	34	80	86	85
La	23	20	25	24	22	21	24	20	23	29	22	11	37	41	43
Nb	28	22	23	22	21	18	23	24	24	28	22	12	29	26	27
Ni	12	12	12	13	12	14	12	12	14	15	13	12	11	10	11
Pb	32	32	32	23	19	28	31	29	34	28	30	4	8	7	6
Rb	277	308	288	293	328	286	295	292	353	310	302	88	329	258	254
Sr	120	99	107	115	108	93	116	100	112	111	115	485	155	130	130
Th	23	21	23	115	22	21	22	20	22	25	21	6	23	22	22
V	19	17	18	21	19	14	22	23	27	27	23	192	61	59	58
Y	15	18	17	20	18	14	15	19	24	24	18	25	37	29	30
Zr	163	155	159	167	105	143	159	160	183	189	164	160	290	287	291
Zn	46	52	53	51	50	39	51	50	59	62	54	76	101	104	104
Cr	90	124	93	101	95	121	116	148	121	103	127	120	80	100	112
As	4	3	6	3	3	2	3	3	4	4	3	2	2	1	1
Cu	9	8	9	6	7	8	7	7	6	7	7	33	5	7	6
Ga	15	17	17	17	17	16	15	15	16	17	16	15	19	20	20
Sc	4	4	5	4	5	3	5	4	5	6	4	24	6	6	7
U	8	9	9	9	8	10	8	10	10	8	10	1	9	9	9
Granite : Maras-Jong granite proper Grey : Grey microgranite dyke															

between Maras-Jong granite and the grey microgranite. Rocks of each unit plot in distinct fields although some overlap occurs between the rocks from the same units. Of particular interest are Pb (gap at Pb = 8-19 ppm), V (V = 27-58 ppm), Zn (Zn = 61-101 ppm) and Zr (Zr = 189-287 ppm). In general, the Maras-Jong granite show a decrease of Sc, Rb, Sr, Th, V, Ba, Ce, La, Zn and Zr with increasing SiO₂. Pb, U, Ni, As and Y show no particular trends. Different trends are shown by the grey microgranite, thus As, Ba, Pb, Rb, Sr, V, Y and to a lesser extent Nb and Th decrease and Cr, Ga, La, Sc, Ni and Zn increase with increasing SiO₂. Zr and Th do not show any regular trend with the SiO₂. The importance of K-feldspar, biotite and plagioclase in the differentiation is evident in the large ion lithophile (LIL) modelling. Inter-element LIL variation diagram for pairs Ba-Sr and Ba-Rb are shown in Figure 5. Also shown in each of the diagrams is the vector diagram representing the net change in composition of the liquid after 30% Rayleigh fractionation by removing K-feldspar, hornblende, plagioclase or biotite. In all diagrams the trends are consistent with fractionation of plagioclase, K-feldspar and biotite. The TiO₂ vs Zr diagram is important in constraining the role of zircon, magnetite and sphene as well as hornblende and biotite during crystallisation (Fig. 6). The vector diagram indicates that sphene, zircon and magnetite are more important in determining the trend of the Maras-Jong granite (modes lack of hornblende). Thus

the crystallisation options for the granite are zircon + sphene, zircon + magnetite, zircon + biotite and biotite + sphene or some combinations of these minerals. The grey microgranite dykes show a different trend which is controlled mainly by sphene, hornblende and magnetite

The Maras-Jong REE profile is plotted in Figure 7. All samples are generally enriched in light rare earth elements (LREE) and depleted in heavy rare earth elements (HREE). The REE pattern of Maras-Jong granite has pronounce negative Eu anomaly indicating plagioclase fractionation. The overall abundance of REE do not show any systematically decrease or increase with SiO₂, implying the profile is not controlled by fractionation of REE-rich accessory phases (allanite, apatite, sphene and/or zircon).

TYOLOGY

The main criteria for distinguishing I and S type granites can be summarized as follows (see Chappell and White, 1992, for a comprehensive review): S-types are always peraluminous [Alumina saturation index, (ASI > 1)] and contain Al-rich minerals (e.g. Al rich biotite, cordierite, muscovite, garnet, sillimanite and andalusite). Chemically they are lower in Na, Ca, Sr and Fe³⁺/Fe²⁺ and higher in Cr and Ni. I-types are metaluminous to weakly peraluminous (ASI < 1.1) and commonly contain biotite, hornblende and sphene. In terms of their isotopic composition, S-type

granites have higher $\delta^{18}\text{O}$ values ($>10\text{‰}$) and more evolved Sr and Nd isotopic composition. I-type granites range in $^{87}\text{Sr}/^{86}\text{Sr}$ from 0.704 to 0.712 and epsilon Nd from +3.5 to -8.9. For the S-type granites, the corresponding values are 0.708 to 0.720 and -5.8 to -9.2. The S-types granites contain a diverse assemblage of metasedimentary enclaves, whereas enclaves in I-types are commonly metaluminous and hornblende bearing. Mineralogy of the granite especially

the presence of garnet and tourmaline suggest that the Maras-Jong granite fall in the S-type granite criteria of the Eastern Belt province. However Na_2O vs K_2O plot (Fig. 8) shows that the Maras-Jong granite plots in the I-type field. This diagram implies that the Maras-Jong granite has high Na_2O content. This is supported by ACNK values, the samples from Maras-Jong granite plot in well below ACNK = 1.1 (Shand, 1943; Zen, 1988).

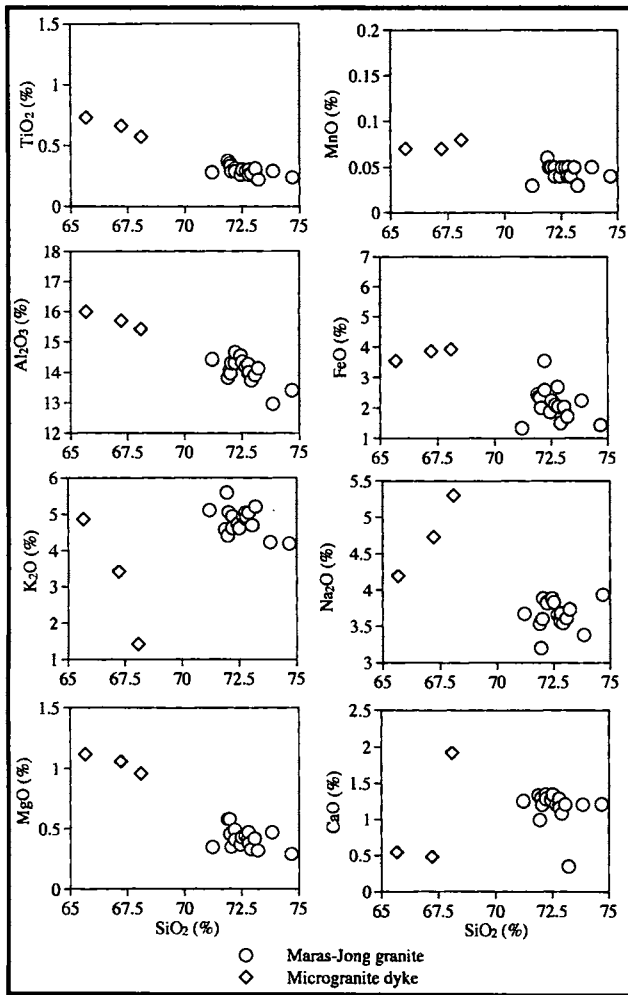


Figure 2. Major elements Harker diagram of the granitic rocks from the Maras-Jong granite.

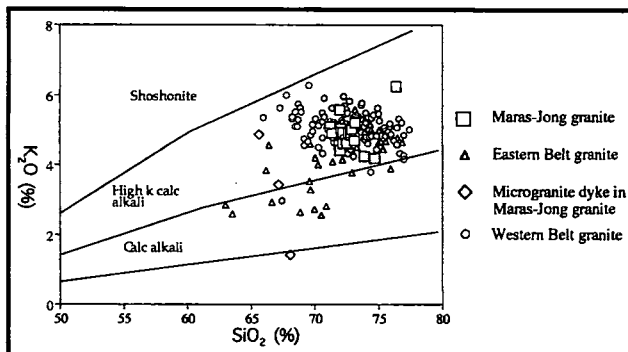


Figure 3. K_2O vs SiO_2 diagram for the Maras-Jong granite and its microgranite dykes. Also plot in the diagram is the samples from both Western and Eastern belt granite.

CONCLUDING REMARKS

The granite is homogeneous and has been intruded by dolerite and grey microgranite dyke magmas. The dolerite dykes are common throughout the Eastern Belt granite (Azman, 2001a, b; Azman *et al.*, 1998, 2001, 2002) and are different in origin from the Maras-Jong granite proper. The grey microgranite dykes are restricted only to the Maras-Jong granite and closely associated with the granite. In K_2O vs SiO_2 plot (Fig. 3) the grey microgranites show a different trend from the Maras-Jong granite proper. The trend grades from calc alkali to high K calc alkali to high-k calc alkali which is clearly not a magmatic trend. Roberts and Clemens (1993) showed that a parent magma with a given K_2O and SiO_2 content will evolve within the particular field in a K_2O vs SiO_2 diagram and for magma to evolve into an adjacent field some process other than crystal-liquid separation must operate. This clearly indicates that the grey microgranites and the Maras-Jong granite are very different and have different sources. This is supported by the fact that the former shows a different trend of much of the trace elements compared to those from the Maras-Jong granite proper.

The granitic rocks of the Maras-Jong granite are texturally similar to the Main range granites. Other characteristics of the Maras-Jong granite that are similar to the Western Belt Granite are presence of tourmaline, garnet and high SiO_2 content (69-77%). Both granites are coarse grained primary textured sometimes dominated by K-feldspar phenocrysts. In some felsic members of the Maras-Jong granite, garnet is found as an accessory phase. Figure 3 show the K_2O vs SiO_2 plot for the Maras-Jong and associated grey microgranite dykes, as well as Eastern and Western belt granites. The Eastern belt samples are more scattered compared to the Western and Maras-Jong granites, thus the latter two have similar K_2O content. The Maras-Jong granite also has higher Rb/Sr ratio (Fig. 9) compared to the Eastern belt granite of similar SiO_2 content. This may lead to conclusions that the Maras-Jong granites is S-type rather than I-type. However the Na_2O vs K_2O plot clearly shows that the granite has high Na_2O and plot in the I-type field of Chappell and White (1992). The fact that Maras-Jong is I-type granite is support by the ACNK values of the rocks i.e all analysed samples have ACNK < 1.1 . Geochemical analyses of the biotite from the Maras-Jong granite also give low Al_2O_3 which is in contrast to the biotite of sedimentary origin which has high Al_2O_3 . Furthermore, REE plot show that the Maras-Jong granite

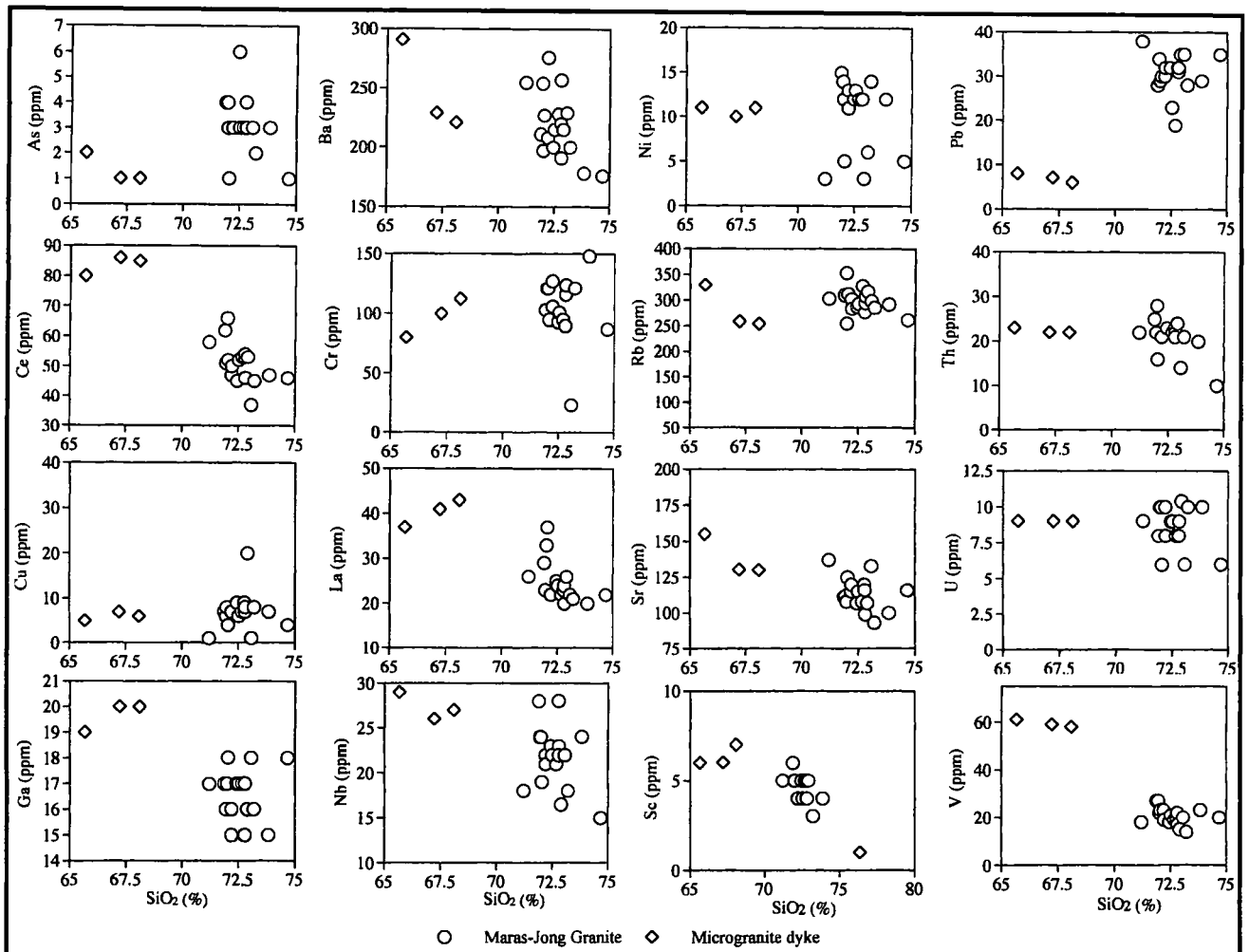


Figure 4. Trace elements Harker diagram of the granitic rocks from the Maras-Jong granite.

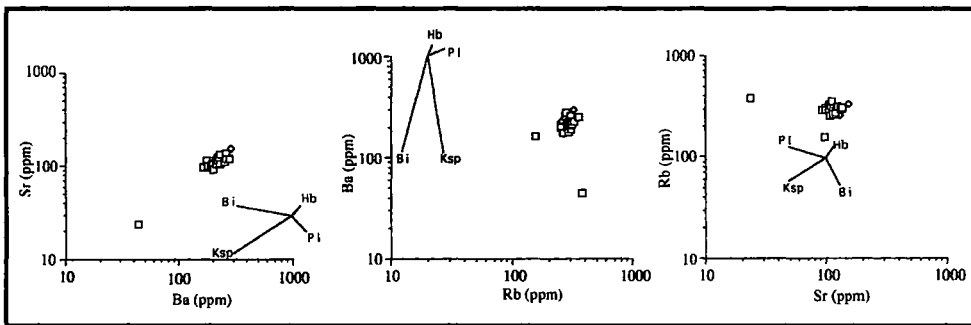


Figure 5. Log-log Ba vs Sr and Ba vs Rb plots of the granitic rocks from the Maras-Jong pluton. Also shown in each of the diagram is the vector diagram representing the net change in composition of the liquid after 30% Rayleigh fractionation by removing K-feldspar, hornblende, plagioclase or biotite.

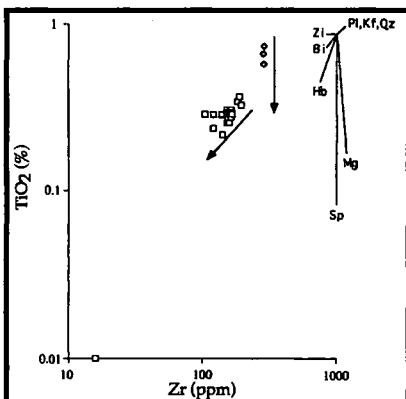


Figure 6. TiO₂ vs Zr log-log plot for the Maras-Jong granite. Mineral vectors indicate path evolved liquids for 15% of a mineral precipitating: Pl: plagioclase; Kf: K-feldspar; Qz: quartz; Mt: magnetite; Sp: sphene; Hbl: hornblende; Bi: biotite; Zi: zircon.

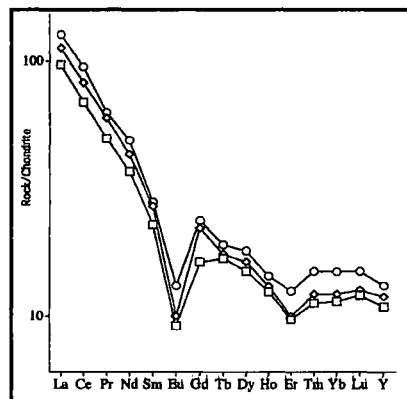


Figure 7. The REE profiles for the granitic rocks from Maras-Jong pluton, Terengganu.

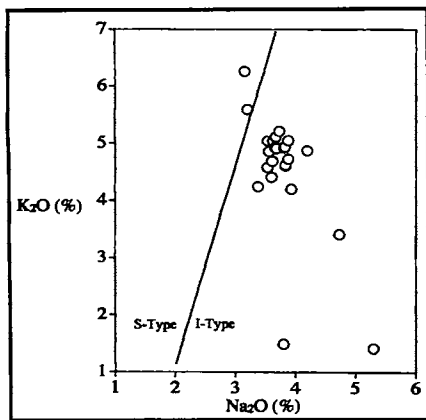


Figure 8. Na_2O vs K_2O plot of the Maras-Jong granite. Field I and S type granite is after Chappell and White (1974).

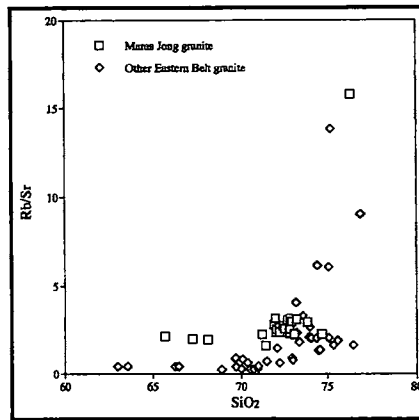


Figure 9. Rb/Sr vs SiO_2 plot of the Maras-Jong granite and the Eastern belt granite of similar SiO_2 . Note that the Maras-Jong granite has slight higher Rb/Sr ratio compared to the rest of the Eastern Belt granite.

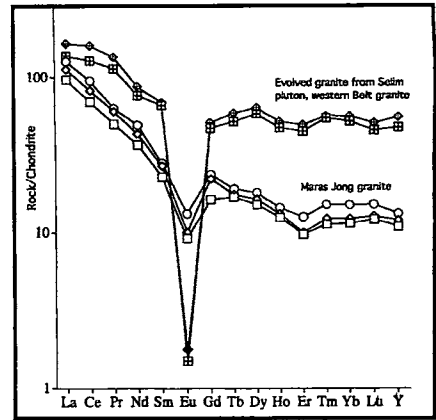


Figure 10. Comparison of the Maras-Jong REE profile and the highly evolved S-type granite from the Western Belt granite.

produce a different profile compared to the highly evolved S-type granite from the Western Belt granite (Fig. 10) (Ludington, 1981, Whalen, 1983, Thorpe *et al.*, 1990, Mohd Azamie & Azman, 2003). Thus although the Maras-Jong granite have many similarities to the S' type granite, the granite is more likely a felsic I-type granite.

ACKNOWLEDGEMENT

This research was supported by University of Malaya grant (FL 0523/98 & FL 0490/ 2001A). The author thanks Prof. Rodney Grapes for the rock analyses at the Department of Earth Sciences, University of Liverpool and to Prof Chen Tingyu for REE analyses at the Chinese National Research Centre of Geoanalysis, Beijing.

REFERENCES

- AZMAN A. GHANI, 2001a. Geochemistry of the mafic dykes from the Eastern Belt (Indochina block) of Peninsular Malaysia. Proceeding International Symposium and Field workshop on the Assembly and breakup of Rodinia and Gondwana, and Growth of Asia, Osaka. *Gondwana Research, (Special issue) Vol. 4(4)*.
- AZMAN A. GHANI, 2001b. Occurrence, subdivision and petrochemistry of mafic dykes from the Perhentian Islands. *Warta Geologi*, 27(3), 73-79
- AZMAN A. GHANI, GRAPES, R. and KHOO T.T., 1998. Geochemistry of dolerite dykes from the Perhentian and Redang islands, Besut Terengganu". *Programme and Abstract GEOSEA 98, Ninth Regional Congress on Geology, Mineral and Energy resources of Southeast Asia*, 214-215.
- AZMAN A. GHANI, KHOO T.T. AND GRAPES, R., 2002. Geochemistry of Mafic dykes from the Perhentian and Redang islands: an example of the younger (dolerite) dykes petrogenesis from the Eastern Belt of Peninsular Malaysia. *Bull. Geol. Soc. Malaysia*, 45, 235-241.
- AZMAN A. GHANI, A TAJUDDIN IBRAHIM, MOHZANI MOHAMAD, WAN ZAKARIA WAN IBRAHIM, REKMAN A. RASHID, WAN SALMI WAN HARUN, ISMAIL YUSOFF, AFANDI MUDA, KAMARUL HADI ROSELEE, AMAN SHAH OTHMAN, ANUAR ISMAIL AND MOHAMAD ALI HASAN, 2001. Occurrence, field relation and petrochemistry of the mafic dykes from Kenyir area, central Terengganu". *Proceeding Annual Geological Conference, Geological Society of Malaysia, 2000*, Pan Pacific, Pangkor, 141-145.
- CHAPPELL, B.W. AND WHITE, A.J.R., 1974. Two contrasting granite types. *Pacific Geol.*, 8, 173-174.
- CHAPPELL, B.W. AND WHITE, A.J.R., 1992. I- and S-type granites in the Lachlan fold belt. *Trans. Roy. Soc. Edinb: Earth Sciences*, 83, 1-26.
- COBBING, E.J., PITFIELD, P.E.J., DARBYSHIRE, D.P.F., and MALICK, D.I.J., 1992. *The granites of the South-East Asian tin belt*. Overseas Memoir 10, B.G.S.
- LIEW, T.C., 1983. *Petrogenesis of the Peninsular Malaysia granitoid batholiths*. Unpubl. PhD thesis, Australia National University.
- LUDINGTON, S., 1981. The Redskin granite: evidence for thermogravitational diffusion in a Precambrian granite batholith. *Jour. Geophys. Res.*, 86(B11), 10423-10430.
- MASON, G.H., 1985. The mineralogy and textures of the Coastal batholith, Peru. In: W.S. Pitcher., M.P. Atherton., E.J. Cobbing and R.D. Beckinsale (Eds.), *Magmatism at a plate edge: the Peruvian Andes*. Blackie Glasgow, 156-166.
- MOHD AZAMIE W.A. GHANI AND AZMAN A. GHANI, 2003. Granitic rocks from Pos Selim-Kampung Raja new road: Petrochemistry of the Selim pluton (CH 0000 to CH 3370). *This issue*.
- ROBERTS, M.P. AND CLEMENS, J.D., 1993. Origin of high-potassium, calc alkaline, I type granitoids. *Geology*, 21, 825-828.
- SHAND, S.J., 1943. *Eruptive rocks*. T. Murby and Co., London, 2nd edn., 444p.
- STRECKEISEN, A.L., 1976. To each plutonic rock its proper name. *Earth Sci. Rev.*, 12, 1-33.
- THORPE, R.S., TINDLE, A.G. AND GLEDHILL, A., 1990. The petrology and origin of the Tertiary Lundy granite (Bristol Channel, U.K.). *Journal of Petrology* 31, 1379-1406.
- WHALEN, J.B., 1983. The Ackley City batholith, southeastern Newfoundland: evidence for crystal versus liquid state fractionation. *Geochemical et. Cosmochim. Acta*, 47, 1443-1457.
- ZEN, E., 1988. Phase relations of peraluminous granitic rocks and their petrogenetic implications: *Ann. Rev. Earth and Planet. Sci.*, 16, 21-51.